Temperature Dependence of the Raman Spectra of Individual Carbon Nanotubes

Zhenping Zhou,*,† Xinyuan Dou, Lijie Ci, Li Song, Dongfang Liu, Yan Gao, Jianxiong Wang, Lifeng Liu, Weiya Zhou, and Sishen Xie*

Institute of Physics, Center for Condensed Matter Physics, Chinese Academy of Sciences, Beijing 100080, China

Dongyun Wan

Laboratory of Nuclear Analysis Techniques, Institute of High Energy Physics, Chinese Academy of Sciences, Beijing 100039, China

Received: June 17, 2005; In Final Form: October 5, 2005

Resonant Raman scattering (RRS) spectra of individual carbon nanotubes on a SiO_2 substrate have been investigated first in the temperature range of 100−600 K (*Phys. Rev. B* **2002**, *66*, 115411). It was revealed by the intensity abnormality of the radial breathing mode (RBM) that the carbon nanotubes have a temperature-dependent density of electronic states. This means that the previously reported temperature coefficients of RBM of carbon nanotubes are smaller than their "real" ones for the bulk samples of single- or double-walled carbon nanotubes. Comparatively, the G line of individual nanotubes shows no observable difference relative to the bulk samples.

Introduction

The discovery of single-walled carbon nanotubes (SWNTs)[1,2] has prompted numerous studies on this new form of carbon to clarify its physical properties in view of potential applications.[3] Resonant Raman scattering (RRS) was shown to be a powerful and nondestructive technique to investigate the electronic properties of this unique one-dimensional system theoretically and experimentally.[4−14] It is well-known that carbon nanotubes have a strong temperature-dependent effect,[15−20] and all the Raman modes, including radial breathing mode (RBM) and the tangential G band, downshift with increasing temperature. The change of phonon frequency with temperature is also valuable in the analysis of Raman spectra, and allows us to investigate the electronic structure and properties of carbon nanotubes. It has been revealed that the temperature dependence of Raman spectra is a direct consequence of anharmonic terms in the lattice potential energy,[21,22] and the volume and temperature effects dominate the change of phonon frequency.

So far, however, all the investigations on the temperature-dependent Raman spectra have focused on bulk samples in which carbon nanotubes with a wide distribution of diameters and different chiralities are present. The resulting spectra generally show a superposition of Raman scattering from all the active nanotubes. This makes it extremely difficult to obtain a correct correlation between the electronic and phonon properties and the corresponding structure of carbon nanotubes. In this paper, isolated individual SWNTs have been prepared and deposited on a SiO_2 wafer through a direct floating catalytic chemical vapor deposition (FCCVD) technique. By using micro-Raman microscopy, the Raman spectra of an individual nanotube have been taken at different temperatures. It was thus revealed that, besides its natural diameter and chirality, the energy difference between the van Hove singularities (vHs) in the conduction and valence bands is also dependent on the surrounding temperature of carbon nanotubes.

* Corresponding author. E-mail: ssxie@aphy.iphy.ac.cn. Telephone: 86-01-82649081. Fax: 86-01-82640215.

† Current address: CEMES−UPR A-8011 CNRS, Groupe NanoMat, BP 94347, France. E-mail: zhou@cemes.fr. Telephone: +33 5 62 25 78 83. Fax: +33 5 62 25 79 99.

Experimental Section

Our FCCVD method for preparing the individual SWNTs has been described in detail elsewhere.[23] Generally, the mixture of ferrocene and sulfur powder was sublimed in the first furnace. A gas mixture of argon and acetylene carried the sublimed catalyst through a narrow connection tube into the roomy reaction zone in the second furnace. The reaction temperature was 1100 °C, and the system pressure was held at 1 atm. The SWNTs thus formed were then deposited on the SiO_2 substrates preplaced in the outer-end section of the reactor. It was found that, by adopting this setup together and adjusting the process parameters, isolated or small-bundle SWNTs were successfully deposited on the Si substrate.[23]

For Raman measurements, a micro-Raman setup (Renishaw RM2000) was used to obtain the Raman spectra, with the 632.8-nm line from a He−Ne laser. The sample-borne substrate was mounted in a cryostat, allowing the sample temperatures to be tuned in the range of 100−600 K with liquid-nitrogen cooling or electrical heating. To minimize the laser heating, a 20× objective lens and a low laser power of ∼0.5 mW were used. The spatial resolution of the instrument is 1 cm^{-1}.

Results and Discussion

Figure 1 shows the variation of the Raman spectra of an individual carbon nanotube as a function of temperature. As expected, the frequencies of all the Raman modes, including RBM and G band, downshift simultaneously with increasing sample temperature, consistent with the previous reports.[14−19] In fact, to obtain the Raman spectra from the same individual nanotube at different temperatures, two steps have been adopted.

10.1021/jp053268r CCC: $33.50
Published on Web 12/24/2005

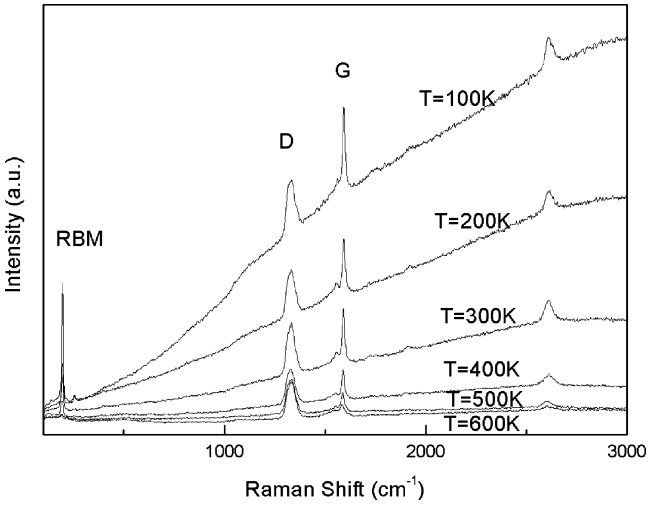

Figure 1. Raman spectra from an individual carbon nanotube as a function of temperatures.

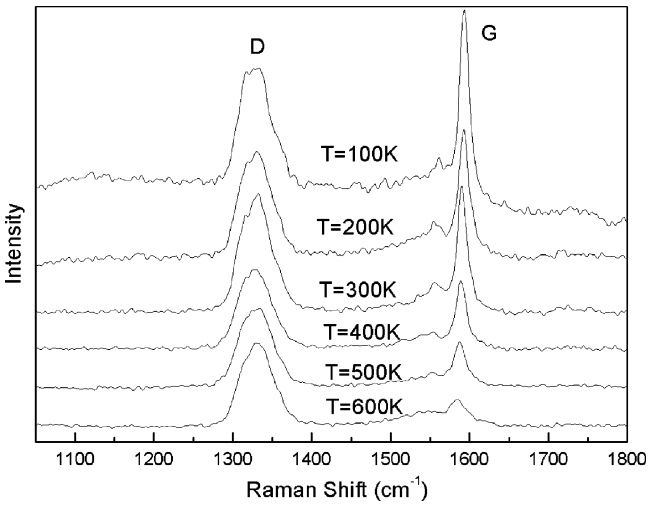

Figure 2. Temperature dependence of the D band and G band for the individual nanotube.

First, samples with a very small concentration of nanotubes on the SiO_2 substrate (about 0.4 tubes per μm^2) have been used. Then, we marked or positioned the individual carbon nanotube with the natural impurity spots on the substrate during the experimental process. Even so, we generally could not acquire the complete Raman spectra in the whole temperature range from 100 to 600 K.

In Figure 2, we show the details of the temperature dependence of the D and G bands of the individual nanotube. Interestingly, the intensity of the G line greatly declines, while the D band shows almost no change in its intensity or its profile with increasing temperature. The intensity difference between the maximum and minimum values of the D band is only about 35%. The variation of the low-frequency RBM (centering at 197.5 cm^{-1} at 100 K) with temperature is shown in Figure 3a. As is observed, the intensity of RBM exhibits a sharp increase at first and then a gradual decrease as the temperature changes from 200 to 600 K, quite different from the situation of the D and G bands. To characterize this intensity abnormality quantitatively, we plotted the relative intensity of RBM in Figure 3b by using the nearly unchanged D mode as the intensity standard at each temperature. The relative intensity of the RBM peak increases until 200 K and subsequently decreases with further increase of the temperature. Ultimately, when the

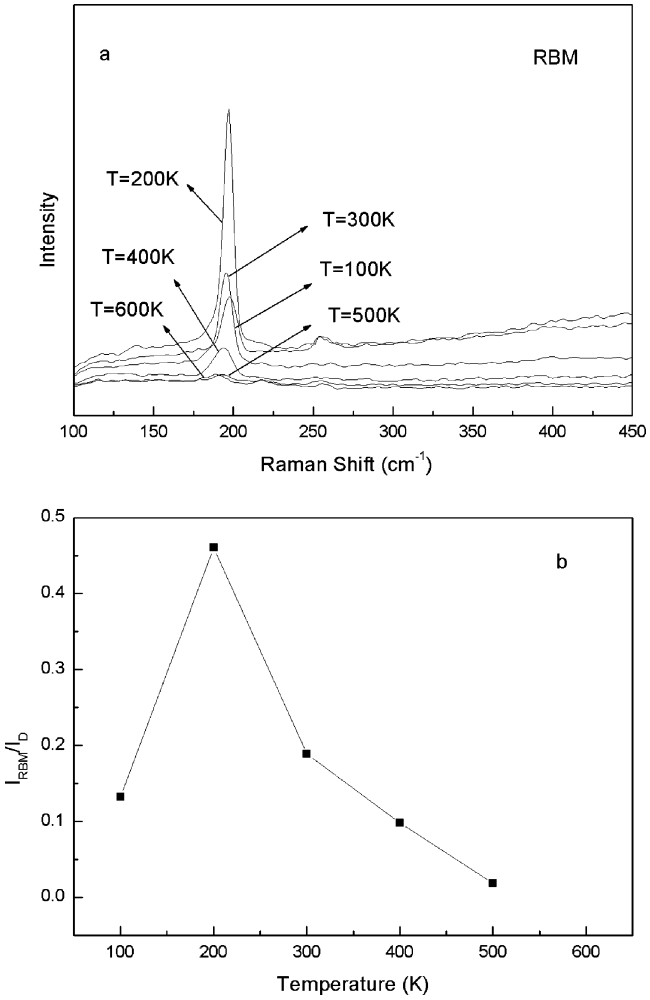

Figure 3. (a) Temperature dependence of RBM for the individual nanotube; (b) the variation of the relative intensity of RBM with changing temperatures.

temperature reaches 600 K, RBM is hardly observable in the Raman spectrum.

This temperature-dependent abnormal behavior for the RBM intensity cannot be ascribed to the length difference of the nanotube exposed under the laser beam when we consider the nearly unchanged D mode and the continually decreased G line. This compels us to turn to other reasons. As has been well established, Raman spectra of SWNTs exhibit a strong resonant behavior.[6,11,24] Resonant Raman scattering will occur when the incident or scattered photon (E_{laser}) matches the interband transitional energy (E_{ii}) between the *i*th van Hove singularities (vHs) in the conduction and valence bands of nanotubes. Under the resonant circumstance, the strong Raman signal can be observed, even in a single nanotube level,[25] just as shown in Figure 1. On the contrary, with the difference between the E_{laser} and E_{ii} energy increasing, this resonant effect will weaken and even completely disappear when E_{laser} is beyond the resonant window of nanotubes.[7] We, therefore, concluded that this abnormal variation of the relative RBM intensity should be correlated with the change of E_{ii} with temperature. This means that the density of electronic states (DOS) of the nanotube is temperature dependent. On the basis of the above assumption, we could further model the experimental resonant Raman process. At 100 K, the nanotube has a slightly greater transitional energy E_{ii} than the excitation laser energy E_{laser}, in which case the resonant scattering is relatively modest. With the temperature raised to 200 K, the E_{ii} becomes smaller, and thus the difference

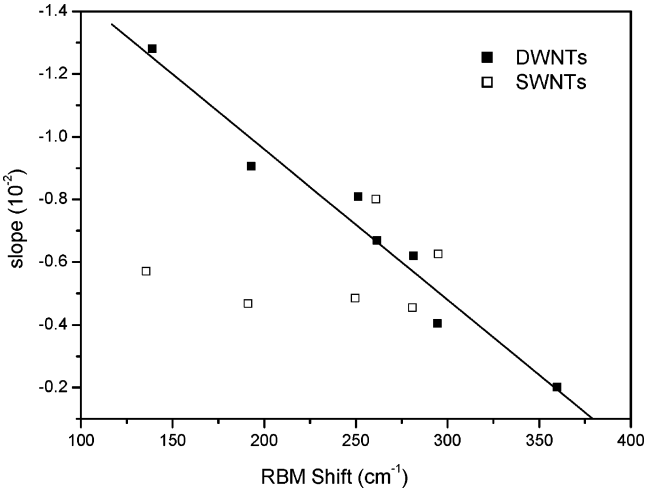

Figure 4. Dependence of the temperature coefficients of RBM of DWNTs on their frequencies, showing a nearly linear decrease with the increased frequencies. The solid line is the linear fit of the Raman frequencies of DWNTs. Comparatively, SWNTs shows almost the same temperature coefficients for different RBM frequencies.

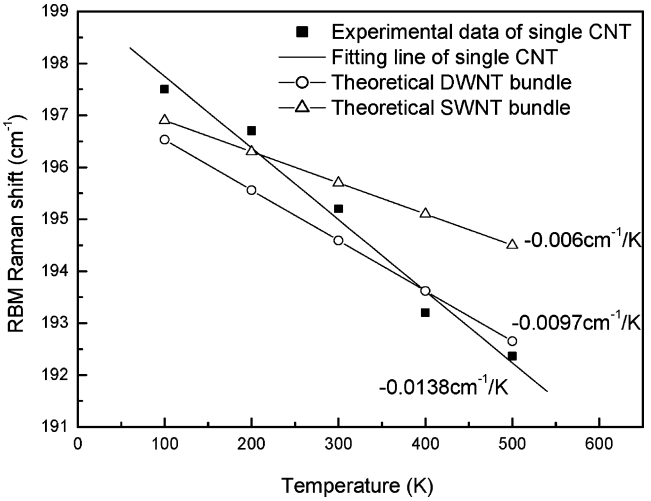

Figure 5. Comparison of the temperature coefficient of RBM between the individual nanotube and the bulk SWNT or DWNT samples. The Raman shift of RBM of the single nanotube shows the faster decrease with temperature.

between E_{ii} and E_{laser} decreases, and they can even become equal. Correspondingly, the scattering cross section of the Raman signal tends to increase, and ultimately, an intensity peak point can be reached just as shown in Figure 3a. Thereafter, the Raman intensity turns back and decreases again as E_{ii} and E_{laser} separate from each other, owing to the excessively increased temperature. Ultimately, the Raman signal cannot be observed in the spectrum.

On the other hand, the above process would lead to smaller RBM temperature coefficients than their "real" ones for the bulk samples if the above conclusion is right. To elucidate this point, we further introduce the temperature-dependent Raman spectra of bulk samples. The common bulk sample can be considered to contain various diameters of carbon nanotubes. At a given temperature (T_1), the Raman scattering will be resonantly dominated by the nanotubes (d_t^1) whose transitional energy (E_{ii}^1) is mostly close to the incident or scattered photon (E_{laser}). However, when the temperature increase to a sufficiently high value (T_2), E_{ii} of all the nanotubes will as a whole tend to a smaller value according to the previous assumption. In these circumstances, the Raman scattering will be dominated by another type of nanotube, which has a greater E_{ii} at T_1 and thus a smaller diameter, according to the inverse relation between E_{ii} and the tube diameter.[3] Ultimately, the RBM frequency thus obtained at T_2 will show a bigger value relative to the "supposed" one as a result of the inverse relation between tube diameters and Raman frequencies, and the slope of the temperature-dependent RBM frequency shows a smaller value.

To validate the above conclusion, we further compared the temperature coefficient of the individual nanotube with those from bulk SWNT and double-walled carbon nanotubes (DWNT) samples. In the previous research, a frequency-dependent temperature coefficient for bulk DWNT samples has been found[26] and is re-plotted in Figure 4. Furthermore, we carried out a linear fitting on this frequency-dependent temperature coefficient (Figure 4), and the following temperature coefficient−frequency relation,

$$10^2 \cdot \alpha = -1.919 + 0.0048 \cdot \omega_{RBM} \qquad (1)$$

has been obtained, where ω_{RBM} is the RBM frequency and α the temperature coefficient of the bulk DWNT samples at the corresponding frequency. Subsequently, with ω_{RBM} in eq 1 replaced by the RBM frequency of the previous individual nanotube at 100 K (197.5 cm^{-1}), the corresponding temperature coefficient of the bulk DWNT samples can be obtained: $\alpha = -0.0097$ cm^{-1}/K shown in Figure 5. In Figure 5, we also give the serial spots of RBM frequencies of the bulk DWNT samples at the corresponding environmental temperature as the individual nanotube based on the above theoretical temperature coefficient $\alpha = -0.0097$ cm^{-1}/K. According to a similar principle, the temperature-dependent RBM frequencies for the bulk SWNT samples were also obtained and indicated in Figure 5. As is obvious from Figure 5, the decrease of RBM frequencies of the individual nanotube with temperatures is more rapid than that of either bulk DWNT samples or bulk SWNT samples, consistent with the previous theoretical assumption. It should also be mentioned here that, for this temperature-dependent RBM difference between the individual nanotube and the bulk SWNT or DWNT samples, the temperature-dependent DOS has been considered to play a central role, although we cannot completely exclude the influence from the intertube interaction such as van der Waals in bulk samples. Finally, it is extremely difficult to determine whether the Raman spectra of the individual nanotube in Figure 1 comes from a SWNT or from a DWNT because the two types of nanotubes are generally coexistent in the samples. However, we are inclined to believe that it is a DWNT based on its closer relation with the bulk DWNTs than with SWNTs in Figure 4. This assertion can also be further confirmed by the temperature-dependent G-band spectra shown in Figure 5.

The Raman shifts of the G lines of the single nanotube and of bulk SWNT and DWNT samples with temperature were also investigated and compared, as is shown in Figure 6. Unlike the situation of RBM in Figure 5, no obvious difference between them has been revealed, and the cause should be ascribed to the difficulty of resolving the G band associated with different diameters of tubes. On the other hand, the abnormal behavior in RBM intensity is not reflected in the G band in Figure 2, implying that the resonant scattering process of RBM and that of the G band do not occur simultaneously. The reason should result from the different profile of the resonant window between RBM and G-band.[8,13]

Finally, we should comment on the effect of the substrate and/or residual catalyst on temperature-dependent Raman

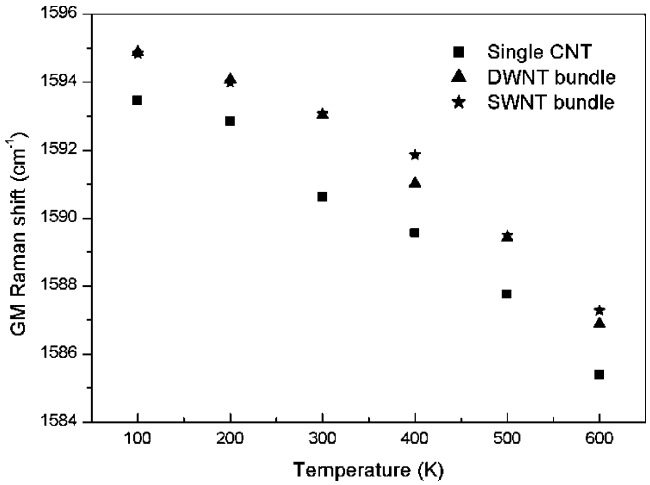

Figure 6. Comparison of the temperature coefficient of the G bands between the individual nanotube and the bulk SWNT or DWNT samples, showing no observable difference.

spectra, primarily due to charge transfer. Charge transfer can strongly affect the temperature-dependent spectra and lead to greater temperature coefficients for the RBM and G bands of SWNT samples.[27] However, in our case, no discernible difference in the temperature coefficients between the individual and bulk samples have been found (Figure 6). This may be due to the fact that nearly each individual nanotube on the substrate is accompanied by one or even more catalyst particles, as was revealed by SEM, AFM, and TEM characterization.[23] Thus the charge transfer, even though occurring, has nearly the same effect on the temperature-dependent spectra of the individual and bulk samples in our case.

Conclusions

We report here the experimental results of resonant Raman scattering performed on the individual carbon nanotube from 100 through 600 K. The relative intensity of RBM shows an interesting peak point with temperature change. We explain this abnormal phenomenon in terms of the temperature-dependent density of electronic states of the nanotube. This process can cause the general temperature coefficient in the bulk SWNT or DWNT samples to deviate to a smaller value, as shown in the previous research. The temperature-dependence of the G band of the individual nanotube was also investigated and compared to that of the bulk SWNT or DWNT samples, and no obvious difference has been revealed.

Acknowledgment. We acknowledge financial support from the National Natural Science Foundation of China and "973" National Key Basic Research. We are thankful for the helpful correction to the paper by P. Hawkes (CEMES, UPR 8011 CNRS).

References and Notes

(1) Iijima, S.; Ichihashi T. *Nature (London)* **1993**, *363*, 603.

(2) Bethune, D. S.; Kiang, C. H.; de Vries, M. S.; Gorman, G.; Savoy, R.; Vazquez, J.; Beyers, R. *Nature (London)* **1993**, *363*, 605.

(3) Saito, R.; Dresselhaus, G.; Dresselhaus, M. S. *Physical Properties of Carbon Nanotubes*; Imperial College Press: London, 1998.

(4) Saito, R.; Dresselhaus, G.; Dresselhaus, M. S. *Phys. Rev. B* **2000**, *61*, 2981.

(5) Popov, V. N.; Henrard, L. *Phys. Rev. B* **2002**, *65*, 235415.

(6) Rao, A. M.; Richter, E.; Bandow, S.; Chase, B.; Eklund, P. C.; Williams, K. A.; Fang, S.; Subbaswamy, K. R.; Menon, M.; Thess, A.; Smalley, R. E.; Dresselhaus, G.; Dresselhaus, M. S. *Science* **1997**, *275*, 187.

(7) Dresselhaus, M. S.; Dresselhaus, G.; Jorio, A.; Souza Filho, A. G.; Saito, R. *Carbon* **2002**, *40*, 2043.

(8) Souza Filho, A. G.; Jorio, A.; Hafner, J. H.; Lieber, C. M.; Saito, R.; Pimenta, M. A.; Dresselhaus, G.; Dresselhaus, M. S. *Phys. Rev. B* **2001**, *63*, 241404.

(9) Souza Filho, A. G.; Jorio, A.; Dresselhaus, G.; Dresselhaus, M. S.; Saito, R.; Swan, A. K.; Ünlü, M. S.; Goldberg, B. B.; Hafner, J. H.; Lieber, C. M.; Pimenta, M. A. *Phys. Rev. B* **2001**, *65*, 035404.

(10) Jorio, A.; Souza Filho, A. G.; Dresselhaus, G.; Dresselhaus, M. S.; Swan, A. K.; Ünlü, M. S.; Goldberg, B. B.; Pimenta, M. A.; Hafner, J. H.; Lieber, C. M.; Saito, R. *Phys. Rev. B* **2002**, *65*, 155412.

(11) Kataura, H.; Kumazawa, Y.; Maniwa, Y.; Umezu, I.; Suzuki, S.; Ohtsuka, Y.; Achiba, Y. *Synth. Met.* **1999**, *103*, 2555.

(12) Rafailov, P. M.; Jantoljak, H.; Thomsen, C. *Phys. Rev. B* **2000**, *61*, 16179.

(13) Jorio, A.; Souza Filho, A. G.; Dresselhaus, G.; Dresselhaus, M. S.; Saito, R.; Hafner, J. H.; Lieber, C. M.; Matinaga, F. M.; Dantas, M. S. S.; Pimenta, M. A. *Phys. Rev. B* **2001**, *63*, 245416.

(14) Jorio, A.; Fantini, C.; Dantas, M.; Pimenta, M.; Souza Filho, A.; Samsonidze, Ge.; Brar, V.; Dresselhaus, G.; Dresselhaus, M.; Swan, A.; Ünlüm, S.; Goldberg, B.; Saito, R. *Phys. Rev. B* **2002**, *66*, 115411.

(15) Huong, P. V.; Cavagnat, R.; Ajayan, P. M.; Stephan, O. *Phys. Rev. B* **1995**, *51*, 10048.

(16) Ruoff, R. S.; Lorents, D. C. *Carbon* **1995**, *33*, 925.

(17) Thomsen, C.; Reich, S.; Goñi, A. R.; Jantoljak, H.; Rafailov, P. M.; Loa, I.; Syassen, K.; Journet, C.; Bernier, P. *Phys. Status Solidi A* **1999**, *215*, 435.

(18) Iliev, M. N.; Litvinchuk, A. P.; Arepalli, S.; Nikolaev, P.; Scott, C. D. *Chem. Phys. Lett.* **2000**, *316*, 217.

(19) Huang, F.; Yue, K. T.; Tan, P.; Zhang, S.; Shi, Z.; Zhou, X.; Gu, Z. *J. Appl. Phys.* **1998**, *84*, 4022.

(20) Li, H.; Yue, K.; Lian, Z.; Zhan, Y.; Zhou, L.; Zhang, S.; Shi, Z.; Gu, Z.; Liu, B.; Yang, R.; Yang, H.; Zou, G.; Zhang, Y.; Iijima, S. *Appl. Phys. Lett.* **2000**, *76*, 2053.

(21) Postmus, C.; Ferraro, J. R.; Mitra, S. S. *Phys. Rev.* **1968**, *174*, 983.

(22) Zouboulis; E. S.; Grimsditch, M. *Phys. Rev. B* **1991**, *43*, 12490.

(23) Zhou, Z.; Ci, L.; Song, L.; Yan, X.; Liu, D.; Yuan, H.; Gao, Y.; Wang, J.; Liu, L.; Zhou, W.; Xie, S. *J. Phys. Chem. B* **2004**, *108*, 10751.

(24) Bandow, S.; Asaka, S.; Saito, Y.; Rao, A. M.; Grigorian, L.; Richter, E.; Eklund, P. C. *Phys. Rev. Lett.* **1998**, *80*, 3779.

(25) Jorio, A.; Saito, R.; Hafner, J. H.; Lieber, C. M.; Hunter, M.; McClure, T.; Dresselhaus, G.; Dresselhaus, M. S. *Phys. Rev. Lett.* **2001**, *86*, 1118.

(26) Zhou, Z.; Ci, L.; Song, L.; Yan, X.; Liu, D.; Yuan, H.; Gao, Y.; Wang, J.; Liu, L.; Zhou, W.; Xie, S. *Chem. Phys. Lett.* **2004**, *396*, 372.

(27) McNeil, L.; Park, H.; Lu, J.; Peters, M. *J. Appl. Phys.* **2004**, *96*, 5158.